JOURNAL OF COMPUTATIONAL PHYSICS 98, 101–107 (1992)

A Numerical Technique for Obtaining the Complete Bifurcated Equilibrium Solution Space for a Tokamak*,†

F. J. HELTON AND J. M. GREENE

General Atomics, San Diego, California 92138-5608

Received September 8, 1989; revised December 18, 1990

This paper describes a new numerical method for finding solutions to the ideal MHD equilibrium problem. The space of solutions thus found can have more than one bifurcation branch, depending on the tokamak being modeled. We suggest that the solutions which are difficult to obtain without the use of this technique correspond to equilibria which are difficult to maintain in the tokamak being modeled. First, this paper investigates, for a tokamak design with large poloidal field-shaping coil (PFC) to plasma distance, the bifurcated numerical solution curve as a function of flux loop position and relates this curve to the practical existence of ideal magnetohydrodynamic equilibria and practical tokamak design. In previous papers, some of the problems which could arise for large PFC-plasma distance were discussed. Then, using a *regularization* technique, it was shown that, for large PFC-plasma distance, the flux loops should be close to the PFCs for stable control if the full information from the flux loops is used. Here it is shown that, for large PFC-plasma distance, the structure of the equilibrium solution space becomes increasingly complex and desirable solutions become more difficult to attain as the flux loops are moved farther from the plasma. In order to explore this solution space numerically, it is necessary to obtain solutions for which the usual Picard iteration method is unstable. Here an extension of this method is given. The solution space is enlarged by adding additional variables and constraints, so that the iteration to the desired solution is stable in the extended space. A modified version of this numerical technique has been used to obtain equilibrium fits to highly elongated DIII-D plasmas. The numerical equilibria are very difficult to obtain without the use of this technique and the plasmas are difficult to maintain in the tokamak.

1. INTRODUCTION

The purpose of this paper is first to investigate, for a typical tokamak design with large poloidal field-shaping coil (PFC) distance, a bifurcated numerical solution curve as a function of flux loop position. The bifurcation properties of this curve can be related to the practical existence of ideal MHD equilibria and practical tokamak design. This study was done for a canonical family of tokamaks at fixed number of PFCs, aspect ratio, triangularity, plasma current, and current profile parameters. Similar bifurcation curves have been addressed in other papers [5, 6].

In earlier work, the viability of a tokamak was discussed in terms of the *first robustness parameter* [1, 2] and the *coil-loop condition number* [3, 4], which are related concepts. The first robustness parameter [1, 2] assesses changes of solution with respect to changes in the current profile. For a given variation in current profile parameter, the *first robustness parameter* was defined to be $(A_p - \Delta A_p)/A_p$, where ΔA_p denotes the maximum plasma cross-sectional area change when the profile parameter is so varied. It is clear that the *first robustness parameter* should be close to 1.0.

The form of the solution space we are exploring depends on the boundary conditions formulated for the partial differential equilibrium equations, Grad–Shafranov equations (GSE) that we study. We incorporate the currents in the PFCs into the equation and solve the GSE with natural boundary conditions at infinity. The currents in the PFCs are determined by the condition that the flux attain certain prescribed values at a number of flux loops.

Control of the plasma then depends on a feedback loop with three links. First, deviations in the plasma current distribution are reflected in changes in the flux at the flux loops. Next, this information is translated into the changes in current in the PFCs needed to restore the flux at the flux loops to the desired values. This is determined with the aid of the matrix of the mutual induction, A, between the PFCs and the flux loops. Finally, changes in the current in the PFCs force restoration of the plasma current distribution back toward the desired state.

In Refs. [3, 4], the second link of this loop was studied and the importance of the second robustness parameter was established. This parameter is the condition number of the mutual inductance matrix A. It is a measure of this sensitivity of the response of the PFCs to changes in values of flux at the flux loops. This link is best behaved when the flux loops and the PFCs are not well separated.

* This is a report of work sponsored by the U.S. Department of Energy under Contract DE-AC03-89ER53277.

0021-9991/92 $3.00

When the flux loops are distant from the plasma, information on the plasma current distribution is degraded at the flux loops. It will be shown here that this can lead to a bifurcation, where there are several solutions all satisfying the same boundary condition. Thus, this paper is concerned with the consequences of the weakening of the first link of the feedback loop.

There are several issues that arise when there are several competing solutions to the same problem. First, the control feedback loop described above will almost certainly be unstable for some of the solutions. Second, when there are several stable solutions, different initial conditions will lead to convergence of the iteration to different final states. The ease of obtaining given desired solutions depends strongly on the range of initial conditions that yield that state. These issues are further treated in Section 3.

Another interesting question is whether the bifurcations of the type found here imply that the physical equilibrium becomes unstable. The physical problem is slightly different since it requires the safety factor profile to be constant during the bifurcation process, while here we require the current profile to be constant. While the two constraints differ, they are sufficiently close to suggest that the ideal $n=0$ stability of these equilibria should be computed.

Thus, it will be seen that, when the PFCs are far from the plasma, the feedback control loop is degraded either in the link between the plasma and the flux loops, or in the link between the flux loops and the PFCs.

The second purpose of this paper is to describe the numerical technique that is used to obtain numerical equilibrium fits to data from elongated DIII-D plasmas. In the analysis of elongated DIII-D shots interesting problems in numerics arise. In particular, at elongations (usually) greater than or equal to 2.4, the numerical iteration schemes used in EFIT and GAEQ do not converge easily to the equilibrium solution consistent with the experimental data. A modification of the technique used to investigate the bifurcated numerical solution curve was used to resolve these difficulties. Preliminary discussion of modern control for tokamaks with highly elongated cross-sectional shape is also included.

In order to obtain all the numerical solutions to a particular ideal MHD equilibrium problem, it is sometimes necessary to modify the basic numerical algorithm while ensuring that the resulting solutions are a solution to the original problem. If such a modification is necessary to obtain a particular solution then the solution must have only a small neighborhood of close solutions and will therefore be difficult to control. Note that for such solutions, the desired solution can be obtained by initializing the current grid with a current grid very close to the solution current grid.

In particular, given the ideal MHD equilibrium problem (Section 2), another variable and constraint is added to the original problem. Then the value of the additional constraint is adjusted to force the value of the additional variable to vanish. The new variable consists of the addition of a nonphysical PFC, a phantom PFC, with a corresponding nonphysical flux loop, a phantom flux loop, and the constraint is the specification of the flux on the phantom flux loop. As the flux value on the phantom flux loop is varied, the current on the phantom PFC varies. For one or more values of flux on the phantom flux loop, the current in the phantom PFC will be 0.0. Each of these flux values then corresponds to a numerical solution to the original ideal MHD equilibrium problem.

2. PROBLEM STATEMENT

Mathematically, the ideal MHD equilibrium problem is: given the elliptic operator

$$L = \Delta^*,$$

$J_\phi(\psi, R)$, I_p, and ψ_i, $i=1, ..., m$, and a finite number of PFCs, find a function ψ and a region A_P with boundary C_P such that

$$L\psi = \mu_0 R\lambda J_\phi(\psi, R) \qquad \text{inside } A_p, \tag{1}$$

$$L\psi = 0 \qquad \text{outside } A_P, \tag{2}$$

except at the PFCs, where it equals the PFC currents to be determined.

The flux function ψ satisfies the boundary conditions

$$\psi = \psi_i \text{ on a set of prescribed flux loops,} \tag{3}$$

$$\psi \quad \text{constant on the boundary } C_P, \tag{4}$$

$$\psi \quad \text{smooth across } C_P, \tag{5}$$

$$\psi = 0 \text{ at infinity,} \tag{6}$$

and the normalization condition

$$\int_{A_P} \lambda J_\phi[\psi(R, Z), R]\, dR\, dZ = I_P. \tag{7}$$

The equation above will be referred to as the Grad–Shafranov equation (GSE).

The current J is nonvanishing only in a simply connected region A_P, in which the flux contours form closed curves. If a level curve of ψ has several disconnected branches, the current is nonvanishing only on one branch. The current depends on the flux ψ through the combination $(\psi-\psi_1)/(\psi_1-\psi_0)$. Thus, the current distribution is fixed as ψ_0 and ψ_1 vary. The quantity ψ_0 is the maximum value of ψ and ψ_1 is the value on the boundary, C_P. For the cases considered here, this surface is defined to be tangent to a prescribed limiting curve. The quantities ψ_0, ψ_1, and C_P differ for

different equilibria, but the limiting surface is fixed. A_P, C_P, and locations $L_1, ..., L_m$ for $\psi_1, ..., \psi_m$ can be seen in Fig. 1.

The space of all solutions that can be obtained from this equilibrium problem is very large. In this calculation, a simplification was obtained by keeping all the parameters constant except the positions and flux values ψ_i assigned to the flux loops. Then the positions of all the flux loops were made to depend on the single parameter ρ' defined below. An equilibrium was calculated for a particular value of ρ' such that the flux loops were at the physical limiter, and the flux values ψ_1 where chosen to be equal so that the equilibrium plasma boundary was close to the physical limiter. In the next section this is called the large volume solution. Then, for different positions of the flux loops, the flux values at the flux loops were chosen so that the large volume solution was reproduced to within numerical error. This is straightforward since the given solution provides values of ψ everywhere, including all the potential locations of the potential locations of the flux loops. This procedure forces each of the families of equilibria that are found to depend on the single parameter ρ'.

A numerical study was performed on an idealized, flexible class of tokamaks. These generic tokamaks (GENEROMAKS) are defined by coils located parametrically according to the expressions

$$x = R_0 + \rho a \cos(\theta + \tau \sin\theta), \tag{8}$$

$$y = \rho a \kappa \sin(\theta). \tag{9}$$

Here, a is the anticipated plasma minor radius and R_0 is the anticipated plasma major radius; κ is the elongation and τ is the triangularity. ρ is a measure of the distance of the surface on which the PFCs lie to the surface which is the physical limiter. For example, $\rho = 2.0$ corresponds to coils at distance $2.0a$ from the magnetic axis. The GENEROMAKS have n coils of the same size, at a distance ρ from the plasma and equally spaced in θ. The GENEROMAKS have m loops of the same size, at a distance ρ' from the plasma and equally spaced in θ. If $\rho' = \rho$ and $m = n$, the loops are at the center of the coils. If $\rho' = 1.0$, the loops are on the physical limiter surface. If $1.0 < \rho' < \rho$, the loops are on a surface between the physical limiter surface and the PFC surface. In Fig. 2, the coil positions at ρ and the loop positions at ρ' are labeled.

The current profile used to obtain the bifurcated numerical equilibrium solution curve was a simple monotone profile with exponential functional form. The results obtained do not depend significantly upon the particular functional form and are similar for any simple monotone profile. The aspect ratio, toroidal magnetic field, plasma current, and triangularity, τ, were fixed.

In this paper, the GENEROMAK studied had aspect ratio 3.0, physical limiter elongation 2.6, and the PFCs were placed on the surface $\rho = 2.4$. The aspect ratio of the physical limiter was constant but the aspect ratio of the solutions varied. The flux loops were placed on surfaces from $\rho' = 1.0$ (physical limiter surface) to $\rho' = 2.4$ (PFC surface). The results with $\rho' = 2.4$ were not included, the results were as expected but numerical convergence of the equilibria was not good. The toroidal magnetic field was fixed at 4.0 T. The ideal MHD equilibrium program used to obtain these results was GAEQ. The calculations were done on the XMP at the MFE center in Livermore. An iteration of GAEQ takes less than a second, these particular equilibria converged in less than 15 iterations (note exception above).

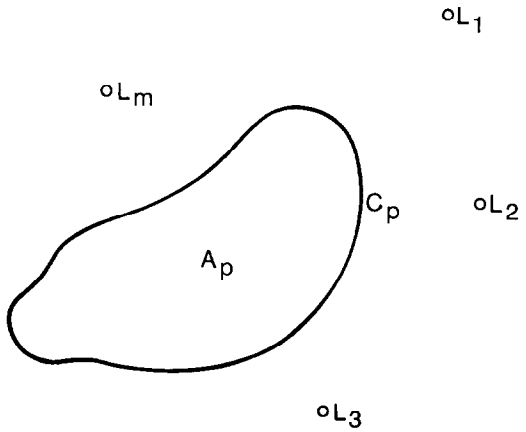

FIG. 1. Region A_P with boundary curve C_P and with flux loops at positions $L_1, L_2, L_3, ..., L_m$ outside C_P.

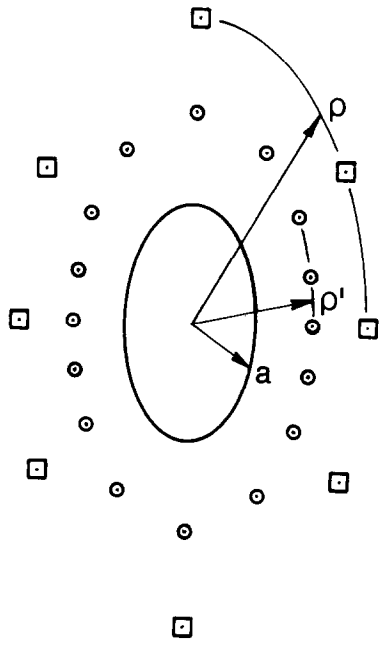

FIG. 2. Example of generomak with PFCs on surface defined by ρ in Eqs. (8) and (9), with flux loops on surface defined by $\rho = \rho'$ in Eqs. (8) and (9).

Depending upon the ρ' used in boundary condition (3) above, the solution space attainable from the resulting numerical method can differ greatly in size and nature.

3. STRUCTURE OF COMPLETE BIFURCATED SOLUTION CURVE

It has been shown [1–4] that the numerical existence of equilibria is a strong function of the plasma–PFC separation, the PFC-loop separation, and the plasma cross-sectional shape. In a numerical simulation, the flux loops can be assumed to lie anywhere between the physical limiter and the PFCs. In this paper it is shown that the size and nature of the attainable solution space is a strong function of the position of the flux loops. In general, the closer the flux loops are placed to the physical limiter, the more sure is the existence of an equilibrium solution having its boundary at that surface. Empirically, in a numerical simulation, if the PFCs are distant from the plasma, then as the position of the flux loops is moved toward the PFCs, additional solutions appear that all satisfy the same boundary conditions.

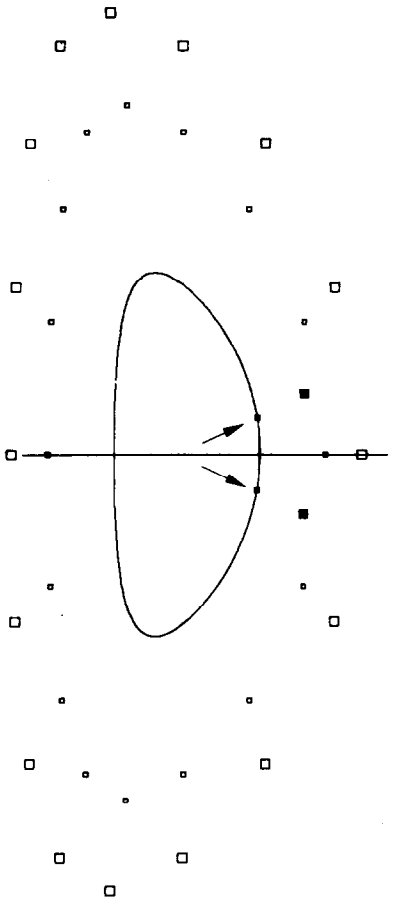

FIG. 3. Example of phantom PFCs and the corresponding phantom flux loops used to obtain the complete numerical bifurcated solution curve for this tokamak. The large squares are the PFCs and the solid black squares are the phantom PFCs. The small squares are the flux loops on the surface $\rho = 1.9$. The small squares with the arrows are the phantom flux loops.

3.a. *Phantom Coils*

In order to obtain all the numerical solutions, it is necessary to introduce a nonphysical PFC [7, 8], a *phantom PFC* with a corresponding nonphysical *phantom* flux loop, each appropriately placed. The numerical technique that is used to find the equilibria depends on starting with an approximate solution and then iterating. There are generally two issues for such procedures. First, is the desired solution a stable fixed point under the iteration? Second, if it is, does it have a large basin of attraction? That is, can this solution be obtained by starting the iteration from a large range of initial conditions? If the answer is negative for either question, the solution will be difficult or impossible to find. In that case, the convergence properties of the iteration can be changed by adding phantom PFCs, together with phantom flux loops. Solutions of the original problem are obtained when a solution is found with vanishing current in the phantom PFC. This is done by iterating on the flux in the phantom flux loop. If the phantom PFCs and flux loops are well placed, they can stabilize, or increase the basin of attraction of these solutions. In the case considered below, there are multiple solutions of the flux at the phantom flux loop that lead to vanishing current at the phantom PFC. Figure 3 shows an example of a phantom PFC used in this paper; the phantom PFC is the closed square, the other PFCs are open squares. The flux loops on the $\rho' = 1.9$ contour are the small open squares and the phantom flux loops are the small black squares indicated by the arrows. The corresponding flux loop is also shown in this figure.

Here, two symmetric phantom PFCs and the corresponding phantom flux loops were used in order to obtain all three solutions for a next generation tokamak. As will be seen in Subsection 3b, this is an example of a dee-shaped

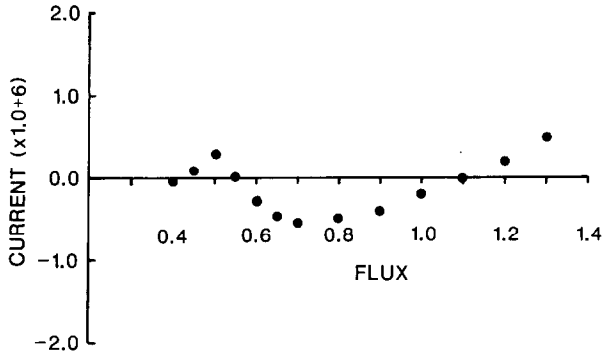

FIG. 4. Sample curve of phantom PFC current versus flux at the phantom flux loop when there exist three bifurcated solutions to the ideal MHD equilibrium problem.

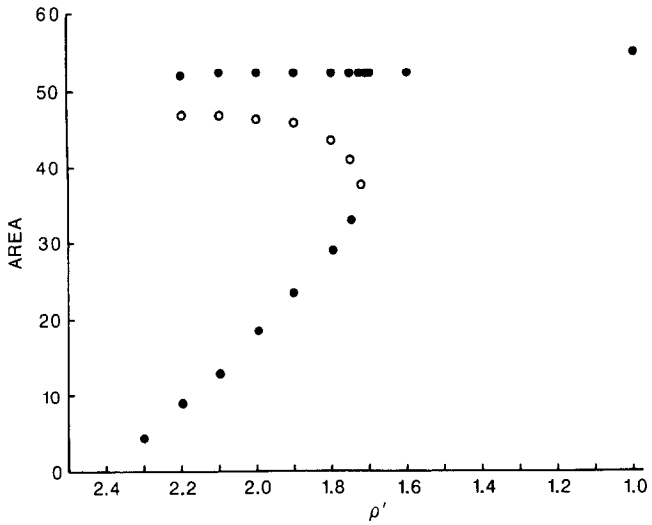

FIG. 5. Structure of the complete numerical equilibrium space for a tokamak with PFC distance $\rho = 2.4$ and limiter elongation $\kappa = 2.6$; ρ' is the distance between the flux loops and the physical limiter.

tokamak with three distinct equilibrium solutions throughout much of its operating space.

3.b. *Structure of Bifurcated Solution Curve for a Given GENEROMAK*

It is shown that a tokamak with limiter elongation greater than 2.0 and with distant PFC systems can have three different types of solutions, a small volume solution, an intermediate volume solution, and a large volume solution. In these calculations, the large volume solution has boundary closest to the physical limiter. Figure 4 shows a sample curve of phantom PFC current versus flux at the phantom flux loop when there exist three bifurcated solutions to the ideal MHD equilibrium problem. When the flux was varied on the phantom flux loop through an appropriate range, one, two, or three equilibrium solutions were found, depending on the position of the flux loops. One of these solutions, the intermediate volume solution, can only be obtained by adding a phantom PFC. The small volume solution is the easiest to obtain numerically, especially when the flux loops are far from the plasma. The large volume solution can be obtained by using an exact current initialization when the flux loops are close to the plasma but it requires the use of a phantom PFC when the flux loops are far from the plasma.

Figure 5 shows the structure of the complete numerical equilibrium space for a tokamak with PFC distance $\rho = 2.4$ and physical limiter elongation $\kappa = 2.6$. Here, the plasma volume is shown as a function of ρ', the distance between the flux loops and the plasma. Note that when the flux loops are close to the plasma, the large volume solution is the only solution and is easy to obtain; this is done by choosing the flux values at the flux loops equal to the same appropriate constant values. When the flux loops are far from the plasma, the large volume solution is close to the unstable intermediate volume solution and therefore difficult to obtain in general. It is difficult to obtain a converged solution of the

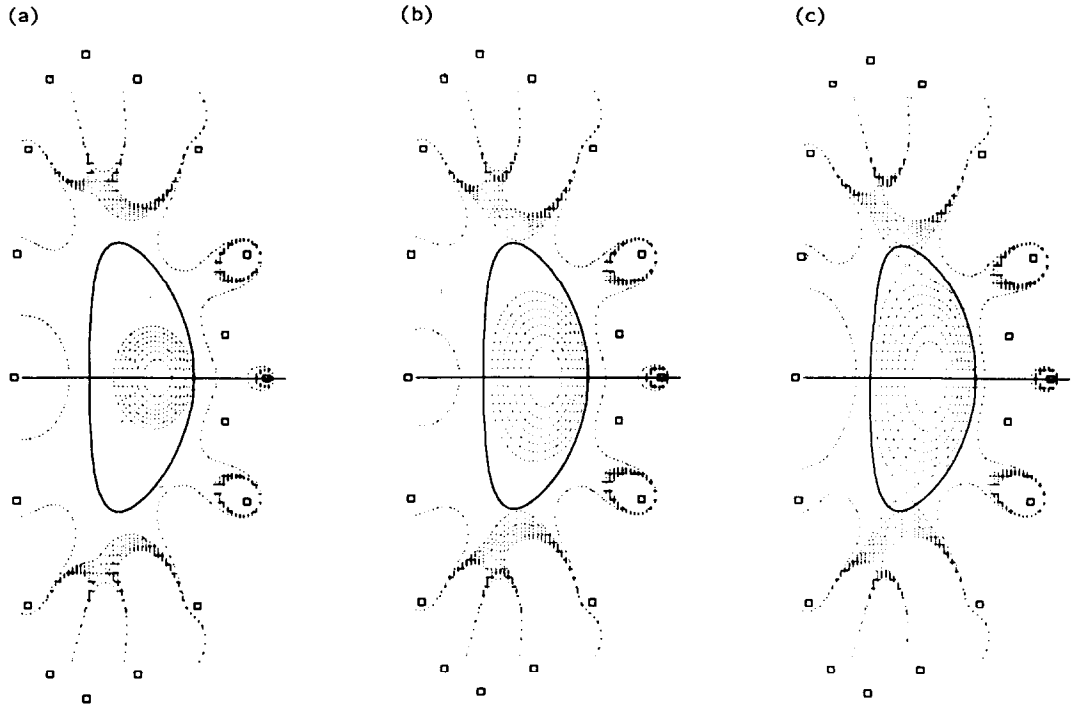

FIG. 6. Examples of the contour plots for (a) small, (b) intermediate, and (c) large volume solution at $\rho = 1.9$. Flux contours outside the plasma have been included in order to provide more information about the solutions.

solution is close to another solution. Here, the flux values at the flux loops are obtained by determining the flux values at these locations in the initial large volume solution. These flux values are interpolated from the initial equilibrium solution when $\rho' = 1.0$. The flux values are, in general, not equal when $\rho' \neq 1.0$. Figure 6 shows the contour flux plots for the small, intermediate, and large solution at $\rho' = 1.9$. The currents in the PFCs, the phantom PFC, and the plasma current are given in Table I. The constant flux value of the $\psi = \psi_i$ is also in the table. The dotted branch is the intermediate volume solution only obtainable with the use of the phantom PFC.

3.c. *Obtaining Numerical Equilibrium Fits for Highly Elongated DIII-D Data*

From the result of earlier [1, 9] numerical experiments, it appears that throughout most of the DIII-D operating space, just one numerical solution exists. Only for non-standard DIII-D plasmas such as highly elongated plasmas does there exist more than one solution. In the analysis of elongated DIII-D shots interesting problems in numerics arise. In particular, at elongations (usually) greater than or equal to 2.4, the numerical iteration schemes used in EFIT and GAEQ do not converge easily to the equilibrium solution consistent with the experimental data. Here, the technique was used to obtain the solution which corresponded to the experimental data.

Figure 7 shows the phantom PFC and the corresponding phantom flux loop used to obtain the elongated equilibrium fits to DIII-D data described in this paper. The DIII-D PFCs and the flux loops are also shown. The currents in the PFCs and the current in the phantom PFC are given in Table II. In this work, the other non-physical solutions were not explored; only the equilibria which fit the experimental data from the DIII-D shots were obtained. The placement of the phantom PFC and flux loop is not restricted but can vary significantly. Certain placements lead to the desired solution more quickly. The placement shown in the figure worked well for all of the experimental cases we considered.

The elongated equilibria are more difficult to control than the less elongated equilibria. Earlier in Ref. [3], the singular values of the inductance matrix were discussed with respect to being able to obtain a particular plasma cross-sectional shape. As expected, with increasingly complex cross-sectional shape more singular values must be kept in the inductance matrix in order to obtain the desired plasma cross-sectional shape. This is equivalent to having to control more plasma parameters. This, although the DIII-D inductance matrix has 18 singular values, a lower elongation dee can be obtained with only seven singular values in the inductance matrix and completely preserve the plasma cross-sectional shape. However, a divertor plasma or highly elongated plasma requires nine or more singular values in

TABLE I

Coil Currents and Plasma Currents for Cases a, b, c in Fig. 6

Volume (cm^3)	23.62	45.01	52.65
ψ_K	0.938	0.558	0.424
I_p	0.40 + 07	0.40 + 07	0.40 + 07
Coil no.	I_p (kA)	I_p (kA)	I_p (kA)
1	0.69 + 07	0.71 + 07	0.72 + 07
ph	0.55 + 02	−0.97 + 02	−0.19 + 02
2	0.17 + 08	0.17 + 08	0.17 + 08
3	−0.36 + 08	−0.36 + 08	−0.36 + 08
4	0.27 + 10	0.27 + 10	0.27 + 10
5	−0.11 + 11	−0.11 + 11	−0.11 + 11
6	0.93 + 10	0.93 + 10	0.93 + 10
7	−0.53 + 09	−0.53 + 09	−0.53 + 09
8	0.50 + 07	0.47 + 07	0.47 + 07

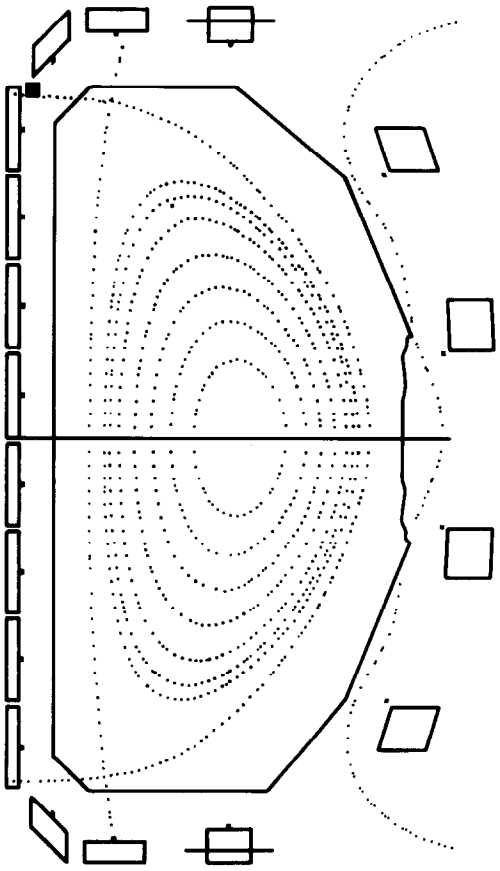

FIG. 7. Example of a phantom PFC (small black square) and corresponding phantom flux loop (small black square with arrow) used to obtain numerical equilibrium fits for highly elongated DIII-D data. The DIII-D PFCs are shown and the small black squares without arrows are the DIII-D flux loops.

TABLE II

Coil Currents and Plasma Currents for the DIII-D Equilibrium Shown in Fig. 7

Volume (cm^3)	20.497		
ψ_K	0.00445	9	−0.83 + 04
I_p (kA)	0.11 + 07	10	−0.25 + 06
1	−0.26 + 06	11	−0.22 + 06
2	−0.21 + 06	12	−0.14 + 06
3	−0.14 + 06	13	−0.28 + 02
4	−0.28 + 05	14	0.18 + 05
ph	−0.21 + 02	15	−0.19 + 06
5	0.14 + 05	16	−0.19 + 06
6	−0.17 + 06	17	−0.29 + 04
7	−0.20 + 06	18	−0.68 + 04
8	0.58 + 04		

the inductance matrix, depending on the complexity of the plasma cross-sectional shape. In addition, with increasing elongation, the $n=0$, $m=1$ mode evolves into the $n=0$, $m=3$ mode [10] which is much more difficult to control.

Figure 7 is an example of a DIII-D equilibrium fit obtained by using the numerical technique described above. In particular, this is S63422 at 2654 ms, note that the elongation is 2.4 the upper triangularity is 0.9 and the lower triangularity is 0.8. This equilibrium has an $n=0$, $m=3$ mode.

Thus, it is expected, that increasing the complexity of the feedback control system on DIII-D will increase the complexity of the plasma cross-sectional shape we are able to control in DIII-D. In summary, the analysis we have done on these experimental shots has indicated certain improvements to tokamak control systems which must be implemented to make future tokamaks with complex highly elongated cross-sectional shapes viable.

4. DISCUSSION

The phantom coil technique described in this paper has been used to numerically obtain equilibria from various solution branches. In both cases, the necessary use of the technique to obtain a particular branch relates (we believe) to the difficulties which would occur in maintaining that solution branch in the experiment.

From the results of earlier ideal MHD equilibrium numerical experiments [1–4] done on GENEROMAKS, it follows that the existence of an equilibrium solution having a desired plasma elongation and triangularity is more certain if the PFCs are closer to the plasma when the plasma is strongly shaped. In order to be sure of obtaining strongly shaped plasmas, the PFCs must be close to the plasma, and conversely, if the PFCs must be far from the plasma, the required plasma cross-section should not be strongly shaped. This was demonstrated in Refs. [1–4], where the importance of the first and second robustness parameters was established.

From the present study, the importance of a third robustness parameter is established, namely the bifurcation number of the solution space. It is apparent that for large PFC-plasma distance of highly elongated plasmas, the structure of the numerical bifurcated equilibrium solution space becomes increasingly complex and desirable solutions become more difficult to attain as the flux loops are moved farther from the plasma. Our results together show that with increasing PFC distance, with increasing plasma elongation and with more strongly shaped plasma cross section, the empirical probability of a robust plasma equilibrium decreases and increasingly severe control problems arise no matter where the flux loops are placed.

All control problems will become more difficult for ignition tokamaks, it becomes more difficult to place poloidal field-shaping coils close to the plasma to shape the plasma, and it becomes more difficult to place a wall close to the plasma to stabilize the low n modes. Also, ignition will lead to unknown current profiles.

ACKNOWLEDGMENT

This is a report of work sponsored by the U.S. Department of Energy under Contract DE-AC03-89ER53277.

REFERENCES

1. F. J. Helton and J. L. Luxon, *Nucl. Fusion* **27**, 887 (1987).
2. F. J. Helton, J. M. Greene, and J. W. Helton, *Comments on Plasma Physics and Controlled Fusion XI, 1987*, p. 127.
3. F. J. Helton, J. M. Greene, and J. W. Helton, *Plasma Phys. Controlled Fusion* **33**, 827 (1991).
4. M. W. Phillips, M. H. Hughes, A. M. M. Todd, J. T. Hogan, R. A. Dory, F. J. Helton, J. M. Greene, J. W. Helton *et al.*, in *Plasma Physics and Controlled Nuclear Fusion Research, Proceedings, 12th Int. Conf. Nice, 1988 (IAEA, Vienna 1989)*, Vol. 2, p. 65.
5. B. Marder and H. Weitzner, *Plasma Phys.* **12**, 435 (1969).
6. H. R. Strauss, *Phys. Fluids* **17**, No. 5, 1040 (1974).
7. F. W. McClain and T. H. Jensen, in *Proceedings, Eighth Conference on Numerical Simulation of Plasmas, Monterey, California, 1978*; CONF-780614, PB6.
8. T. S. Wang, General Atomics, personal communication, 1979.
9. F. J. Helton, L. C. Bernard, and J. M. Greene, *Nucl. Fusion* **25**, No. 3, 299 (1985).
10. F. J. Helton *et al.*, Ideal MHD properties of Elongated DIII-D shots, *Bull. Am. Phys. Soc.* **34**, 2118 (1989); E. A. Lazarus *et al.*, Axisymmetric stability in DIII-D, *Bull. Am. Phys. Soc.* **34**, 1940 (1989).